Chapter IV

White-appearing structural color in the wings of butterflies belonging to *Lepidoptera* order but diverse sub-families and their water-repellency features

The macroscopic objects, which exist all around us, invariably catch the attention of the bystanders due not only to their intrinsic physical make-up but also to their apparent color that reach our eyes. Without color, most of the structures would become indistinguishable. The colour that we see in an object is essentially due to its pigmentary constituents and microstructural make-ups responsible for precise light-matter interaction which undergoes interference and scattering processes at large. The role of micron to sub-micron scale geometrical construction in the determination of color, termed as "structural color" is quite prominent in numerous bird feathers, insect covers, aquatic species and butterfly wings [1]. Butterflies are universally attractive as they come with myriads of bright, iridescent colours and patterns [1,2]. The wings exhibit strong iridescence property as a consequence of diffraction, [3] multi-layer interference [4] as well as photonic crystal effect [5].

The butterfly wings, to a great extent, comprise of chitinous scales, melanin and pterin species which form an integral component of the microstructural patterns and hierarchical units. The epicuticular chitin layer together with distributed air pockets are termed as, '*pepper-pot structures*' [6]. Usually, the butterfly wings are evolved with two kinds of scales of several micrometer length, namely, basal and cover scales. While the basal scales are found to lie directly above the wing lamina, the cover scales just overlay these. The precise evolution of natural construction within the assembly of scale components that includes, ridges, cross ribs, flutes, scutes, *trabeculae* etc., largely account for the ensuing structural coloration [2,7]. Often, a butterfly scale is thought of as a sack consisting of lower and upper laminae [1,7]. Some butterfly wings have multilayer thin film like structure which is capable of producing bright colourful iridescence responses from the reflected sunlight [8]. The lower lamina is joined to the upper lamina, by what is called as, *trabeculae*. While the lower lamina is a thin-film element, the stacking serves as a means for achieving bright colouration [9]. The alteration of structural coloration can be realized due to a varying assembly of the scale components and also due to the refractive

index (R.I.) of the surrounding microstructure [10]. It is believed that, the butterfly scale microstructures could offer natural test-beds to exploit camouflage, display, signalling, thermoregulation etc [11]. In the recent past, substantial effort has been made to exploit the occurrence of iridescent blue coloration in the *Morpho*- and other butterflies [1,12,13]. The iridescent blue coloration in the butterfly *Hypolimnas Salmacis* was shown to be caused by lower thin lamina in the white cover scales and eventually, by way of precise scale stacking [14]. Furthermore, Shevtsova *et. al.* have studied the structural color in the transparent wings of small *Hymenoptera* and *Diptera* [15]. Here the thin wings tend to reflect vivid colors by virtue of wing interference pattern (WIP), which is also responsible for visual signaling as a means of biological significance. Despite the fact that, different colour make-ups were discussed for diverse orders of butterflies within a class, [12-16] the origin of white colour in the wings has not received considerable attention and is rarely discussed in literature [2]. With a focus on white-appearing wing parts, the present work discusses origin of structural colour displayed by three important butterfly specimens of same *Lepidoptera* order but belonging to different sub-families.

Apart from reflectance features, the de-wetting phenomena in butterflies have also attracted the attention of researchers. Butterflies with their dazzled wings are observed to fly in rain. The butterfly wings are known to be composed of chitin, which has the waxy nature, this imparts some kind of hydrophobicity to the wings. But apart from that, the microstructural morphology of the butterfly wings attribute to the water-repellency properties [17].

In this work, micro-morphological architecture and reflectance characteristics with and without ethanolic treatments are being discussed while emphasizing different white-parts of different wing-types. Emphasis is also given to analyze polarization sensitive and angle dependent reflectance responses. A plausible explanation based on surface microstructure linked reflectance as well as conditions responsible for manifestation of structural colouration are also highlighted. Also, the wetting–dewetting features are

studied in butterfly specimens with respect to static and dynamic contact angle measurements.

4.1 Specimen collection and treatment

The samples chosen are essentially wings of the butterflies available in the Indian subcontinent. For instance, the white admiral butterfly (WA, *Limenitis Camilla*) of the *Nymphalidae* family comes with the wings offering alternate white and brown patches, the large-white butterfly (LW, *Pieris Brassicae*) of the *Pieridae* family bears the whole white wings and finally, the dark- blue tiger butterfly (DBT, *Tirumala Septentrionis*) belonging to *Nymphalidae* family offers transparent white-spots embedded in the black wing background. Typically, they possess an average tip-to-tip dimension of ~64 mm, ~58 mm and ~80 mm; respectively. The butterfly specimens were collected from different locations of the garden street within the ring road of our university campus. The forewings of the WA butterfly were sectioned just after its natural death and the white and brown segments were preserved in separate chambers. Similarly, the forewings of the LW and DBT butterflies were collected and sectioned as desired. The digital images of the butterflies under study can be found in Figure 1. In order to make them dirt free, the wing specimens were subjected to mild air blowing prior to further processing and characterization. The sectioned specimens were later dipped in analytical reagent (AR)-grade ethanol (*R.I.*=1.36) and left undisturbed overnight.

Figure 4.1: Digital photograph of (a) White Admiral butterfly (*Limenitis Camilla*), (b) Large White butterfly (*Pieris Brassicae*), and (c) Dark Blue Tiger butterfly (*Tirumala Septrentrionis*) samples.

4.2 Microstructural analyses of the butterfly wing scales

The butterfly wing scales are known to possess complex architecture with the scale components comprising of longitudinal ridges, cross- ribs, scutes, flutes, beads and trabeculae [9, 10]. Most of the wings have these features, but they appear with varying geometry, distribution and slant. The SEM micrographs of the brown and white parts of the WA butterfly, the whole-white area of the LW

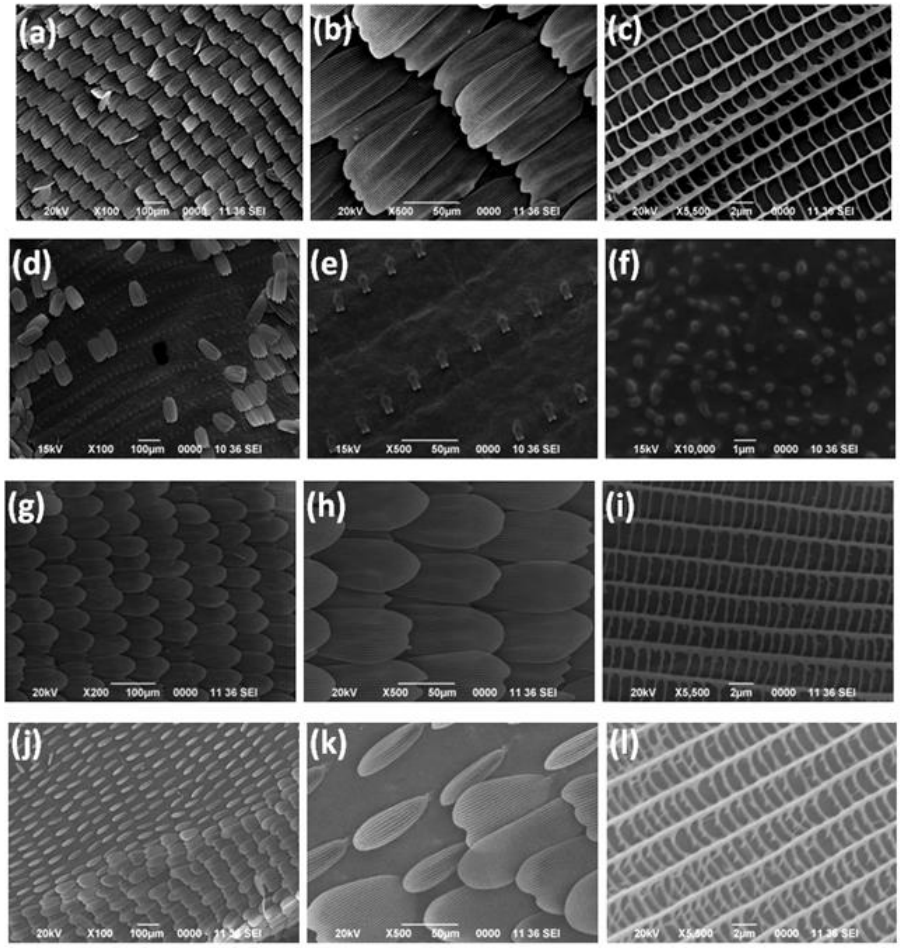

Figure 4.2: SEM micrographs of the (a-c) brown, (d-f) white parts of the WA butterfly wing at different magnifications. While well-ordered scales are evident in the brown part, the white one is devoid of scales at their roots but comprise of micro-bead.

butterfly and the white-spotted area of the DBT butterfly wings are depicted in Fig. 4.2(a-l). The presence of both cover and ground scales, arranged in the form of roof-tiles, can be noticed in the micrograph of the brown part of the wing (Fig. 4.2(a, b)) [18].

Here, the basal scales lie directly above the wing lamina and the cover scales overlay on these. The brown part of the wing is made up of numerous arrays with uniformly distributed scales on it. At a higher magnification, one could easily view the presence of the microscopic, intra-scale components (Fig. 4.2(b, c)) [12]. The scales, as indicated by arrows, are essentially chitinous layers arranged distally across each of the dorsal and ventral wing surfaces [12]. Whereas the longitudinal ridges are aligned parallel to the wing surface, the cross ribs are partly tilted to the longitudinal ridges. The physical parameters of the scale constituents are assessed with the help of *ImageJ* software®. While the scales span over an area of ~4896 μm^2; the average width of the longitudinal ridges within is approximately, 0.35 μm. The average spacing between these ridges is, ~2.7 μm and that of any two cross ribs is, ~1.31 μm.

The appearance of white colour in natural systems is quite interesting. Usually a non-absorbing or pigmentless structure gives white colour [19]. Morphologically, as compared to the brown part, herein, micrographs of the white part of the forewing, gave a distinctive view of the scales. While featuring randomly spread of the scales, the periodic arrangement was seen to be lost completely in the whitish part of the wing. Nevertheless, an array of the actual scale roots can be evidenced from the line-demarcation found in the micrograph (Fig. 4.2 (d, e)). Interestingly, at a higher magnification, several bead like micro-structures are witnessed on the wing surface, unlike the brown part which may have beads at the lower lamina (Fig. 4.2(f)). The typical dimension of the micro-beads was in the range, ~0.35-0.50 μm but with undeniable shape variation [20].

The forewing of the LW butterfly, as can be observed from the SEM micrographs, reveals well-organized scales on the wing surface (Fig. 4.2(g, h)). The magnified images clearly exhibit scales and intra-scale components (Fig.

4.2(h, i)). The width of the cover scales is ~47.3 μm, whereas, the separation between the longitudinal ridges is approximately, 2.8 μm. Moreover, the average thickness of the ridges and spacing between any two cross ribs are estimated to be, ~0.28 μm and 1.26 μm; respectively. We notice ample unfilled space in the rectangular networks formed out of the longitudinal ridges, without any indication of bead like structures. Unlike the other two specimens, in DBT butterfly wings, we observe transparent white spots embedded in the black-bluish background (Fig. 4.1). While the wing comprises of both thin and thick scales, a further inspection of the wing offered a complex architecture of the cross ribs (CR), connecting the longitudinal ridges (LR) at large (Fig. 4.2(j-l)). As an important observation, a periodic distribution of isolated scales as well as stack with scales of varied widths could be visualized from the micrographs.

The width of the thick scales present in the DBT wing is nearly, 48.2 μm and that of the thin scales is approximately, 20 μm. The average thickness of the longitudinal ridges and separation between the cross ribs are measured as, ~0.23 μm and 1.41 μm; respectively. The physical dimension of the intra-scale elements are enlisted in Table 4.1.

After a close inspection of the butterfly wings of WA (*Limenitis Camilla*), LW (*Pieris Brassicae*) and DBT (*Tirumala Septentrionis*) family, one could notice a dull, non-sticky feature in the first kind. The second kind gave a shiny lustre along with noticeable white powdery substance, which tends to come off easily on touch. It is worth mentioning here that, the *Pierid* butterflies essentially possess pterin pigment which is largely responsible for its whitish appearance [21, 22]. Since the LW wing-type belongs to the *Pierid* family it is believed to have evolved with sufficient pigmentary elements. The WA and DBT butterfly wings, however, have no powdery substance, thus indicating the appearance of striking white coloration in these cases is chiefly due to their specific microstructural build up.

Table 4.1: Microstructural parameters of the wing scales obtained through SEM analyses

Sl. No.	Specimen butterfly	Scale distribution	Separation between LR (μm)	Thickness of LR (μm)	Separation between CR (μm)	Bead size (μm)
1	White Admiral (WA)	Periodically arranged (brown) and Random distribution with micro-beads (white)	2.7±0.50	0.35±0.12	1.31 ± 0.2	0.35-0.50 (white)
2	Large White (LW)	Periodic distribution with smoothly packed scale components	2.8± 1.58	0.28±0.09	1.26 ±0.52	No beads
3	Dark Blue Tiger (DBT)	Thin and thick scales are found. Thin scales are loosely packed, thick scales are closely packed	2.75 ±1.9	0.23±0.16 0.43±0.13	1.41±0.2	No beads

4.3 Reflectance spectra of the butterfly wings soaked in ethanolic media

Earlier the white color was believed to be as a consequence of reflectance response of all possible wavelengths of light, mixed in definite proportions and caused by multiple scattering events [23]. The white coloration normally appears opaque or transparent, depending on the thickness of scattering entities that make-up the whole structure. Essentially, the opaque whiteness is the result of scattering from dense bodies. Nevertheless, natural systems (e.g., house and fruit flies) have extremely thin layers, which exhibit white colouration due to non-specific reasons under optimal conditions and in this regard, concept of evolutionary optimisation has been proposed [23]. Yoshioka *et. al*. have made a detailed study on all parts of the wing, including the wing substrate of the *M. Cypris* wings [24]. To understand the color pattern of the wing substrate, the

scales were dipped in PVA solution and consequently, the spectral shape of the reflectance and the emergence colors were analysed. Interestingly, in spite of a large peak in the blue wavelength regime, the white stripes are seen to be quite brighter. Moreover, the blue light was believed to be reflected into a narrow beam that can be comprehended only at a particular angle of observation [24].

Our main motive behind this work was to examine the origin of whitish appearance qualitatively as well as discolouration effect in three specified butterflies belonging to *Lepidoptera* order. The reflectance spectra of the untreated and ethanol- treated wings of the three kinds of butterflies are presented in Figure 4.3(a-h). As a general trend, the reflectance curves of the LW and WA butterfly wings, exhibited a steady growing trend with traces of discontinuities in different ranges of wavelength. A small hump located at ~250-280 nm is attributed to the naturally occurring chitin species present in the wings [4]. The traces of the untreated brown and white parts are depicted in Fig. 4.3(a), with the white one offering a stronger overall reflectance. The apparent white was believed to be evolved with the micron scale-beads, which act as suitable light scatterers, in consistency with the proposition of Stavenga *et.al* [20]. This gives a clear insinuation that, it is not only the geometrical construct but also additional scattering entities present in the microstructure would largely contribute to the displaying of apparent white colour. In order for light scattering events to occur, the bead dimension of the order of hundreds of nanometers is invariably optimized [25]. Owing to a substantial difference in the refractive indices of the chitinous scale and the air gaps, an observably strong reflectance feature (over the visible band) could give rise to a seemingly white appearance, with minimal pigmentary contribution [25]. Moreover, in the spectral region 400-650 nm, a radical improvement in the overall reflectance has been realized in case of the ethanol-treated brown and white parts of the WA wing-parts (Fig. 4.3(b)). This improvement, as a result of ethanol immersion, is ascribed to the filling of micro- voids and air gaps and consequently, momentary suppression of microstructure roughness. The observation of an intense, broad

peak at ~509 nm signifies manifestation of the optical response of the wing scale owing to ethanolic adsorption into the air pockets, thus altering the *R.I.* of the surrounding environment. Owing to the percolation of ethanol into the air gaps and pockets, the *R.I.* difference between the chitinous make-up and its immediate surrounding is invariably lowered. Accordingly, the ethanol-treated brown and white parts of the wing, though vary in strengths, offered quite similar reflectance curves as compared to those of the untreated ones (Fig. 4.3(a, b)). In other words, adsorption of ethanol into the tiny pockets and air gaps of the scales and ridges would confiscate the existence of microstructural network temporarily.

At this juncture, one can say that, the overall reflectance response is mostly due to the surface adsorbed constituent present in the wing parts. Referring to the treated parts, and corresponding to the peak maxima at ~509 nm, the respective reflectance values of the white and brown parts are, ~43.5%, and 33.8%. The notable improvement in spectral characteristics due to ethanol-treatment on individual wing-parts can be found in Fig. 4.3(c, d).

On the other hand, the LW butterfly wings exhibited a reverse trend. The ethanol-treated wing part, particularly in the higher wavelength range, exhibited a lowered reflectance as compared to the untreated counterpart (Fig. 4.3(e)). In the wavelength regime > 400 nm, the reflectance value drops from ~67.5% to 44.7%. The weakening of reflectance realized at higher wavelengths might account for adequate diffuse scattering events, which are more likely for non-smooth surface structure. The DBT butterfly wing also reveals a reverse trend, with the treated wing characterizes a suppressed reflectance as compared to the untreated one that predicts a progressively growing trend in the visible and NIR region. In the visible wavelength regime, nearly two fold drop in the reflectance response is evident after ethanol-treatment. A series of reflectance curves attributed to the investigated parts, before and after ethanol uptake, are shown collectively in Fig. 4.3(g) and (h); respectively. With a different outlook,

structural coloration in uni and multi-coloured butterfly wings and principle of Ag^+ uptake by scales are discussed in a recent work [26].

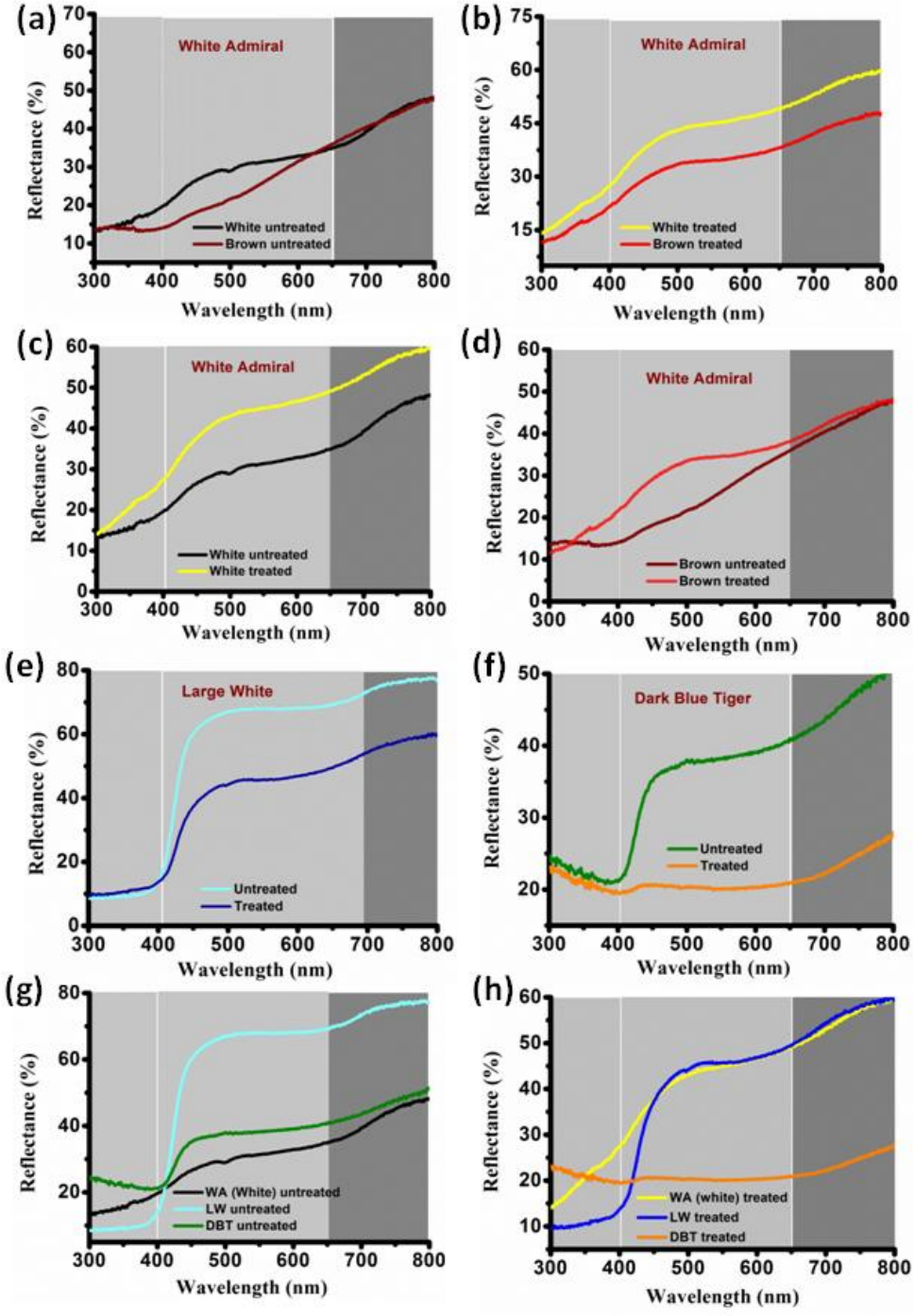

Figure 4.3: UV-visible-NIR reflectance spectra of (a-d) the white and brown parts of the WA butterfly wings, without and with ethanol treatment. The corresponding spectra of the LW and DBT butterfly specimens are presented in (e) and (f); respectively. For comparison sake, as regards untreated and ethanol treatment, the spectra of different whitish parts of all the wing types are plotted together and shown in (g) and (h); respectively.

Despite the fact that, the butterfly wings have whitish appearance in part or whole of the wing, immersion in ethanol gave noticeably altered features owing to diverse micro-morphological build-up that comprises of intra scale components and gaps. Interestingly, *Pierid* butterflies get their superbly whitish gaze from adequate pterin pigments [22]. These organic species are composed of heterocyclic compounds with keto and amino groups. Since chitin-rich elements are amply available in the wings and that they constitute strong scatterers in nature, [23] here, structural white coloration is profoundly manifested by its built-in architecture. The extent of whiteness depends on the extent and kind of light scattering events which may occur via two dimensional intra scale elements and surface structure present in the wing scales.

The transmittance spectra (Fig. 4.4A) of the three specimens are assessed and are compared with the reflectance spectra. For all the three cases, it has been observed that the transmittance response is less than the reflectance, which gives us an idea that colour we see in these wings is largely due to their morphological surface make-up.

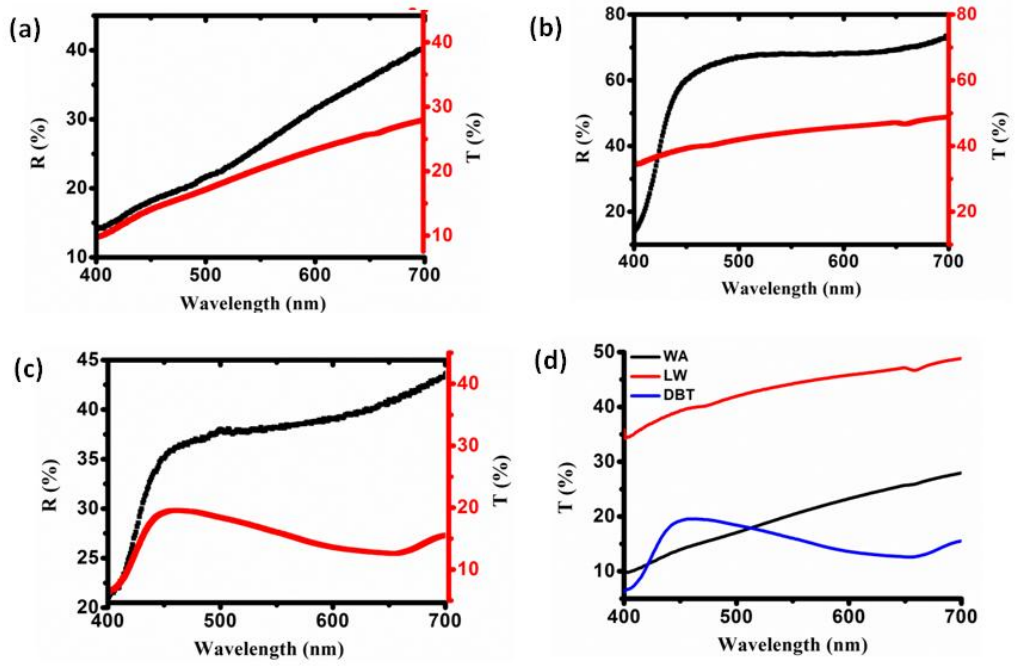

Figure 4.4A: Transmittance and reflectance spectra of the (a) WA, (b) LW, and (c) DBT butterfly wing specimens. All the spectral responses wrt transmission property are plotted together in sub-figure (d).

4.4 Reflectance features w.r.t variable incident angle and polarisation sensitivity

The angle dependent study is important in the sense that one can adjudge viewing angle dependent appearance of the object under study. The consideration of angle dependent reflectance has led to the additional information needed to explain underlying scattering mechanism exhibited by the cover scales and assemblies thereof. For instance, Siddique *et.al.* have reported the iridescent blue coloration in *Hypolimnas Salmacis* wings, and have assigned the origin of blue color to the stacking of black and brown scales [14]. In *Morpho Menelaus* wings, the angle modified discolouration effect was believed to have caused by adequate variation in optical thicknesses through the chitin and air gaps [27].

The reflectance characteristics of the wing-parts in responses to the variation in the wavelength and incident angle can be found in both the 2D and 3D plots, shown in Fig. 4.4B (a-c). Apparently, the specimens offer a higher reflective feature at higher wavelengths and corresponding to a finite incident angle. In reference to the noticeable band maxima at, ~509 nm, a growing reflectance trend has been witnessed with an increasing angle of incidence (Fig. 4.4B (a,b)).

In the 3D view, the series of curves corresponding to varied angles of incidence gives the impression of flapping of bird wing feathers. To be specific, as we change the incident angle from 15°to 75°, the reflectance curves shoot up gradually over the whole spectral region. Since the several micro-beads present in the WA wing specimen act as scattering entities, their reflective power would alter with the angle of incidence substantially. Consequently, contribution via sub-surface volume scattering events is seemingly prominent even though multi-layer interference effects cannot be ignored completely. Earlier, as for the LW butterfly wing [2], a broadband reflectance with a higher reflectivity was noted in the visible and NIR regions (Fig. 4.4B (b)). Moreover, the reflectance response, particularly, in the visible region is independent of the angle of incidence.

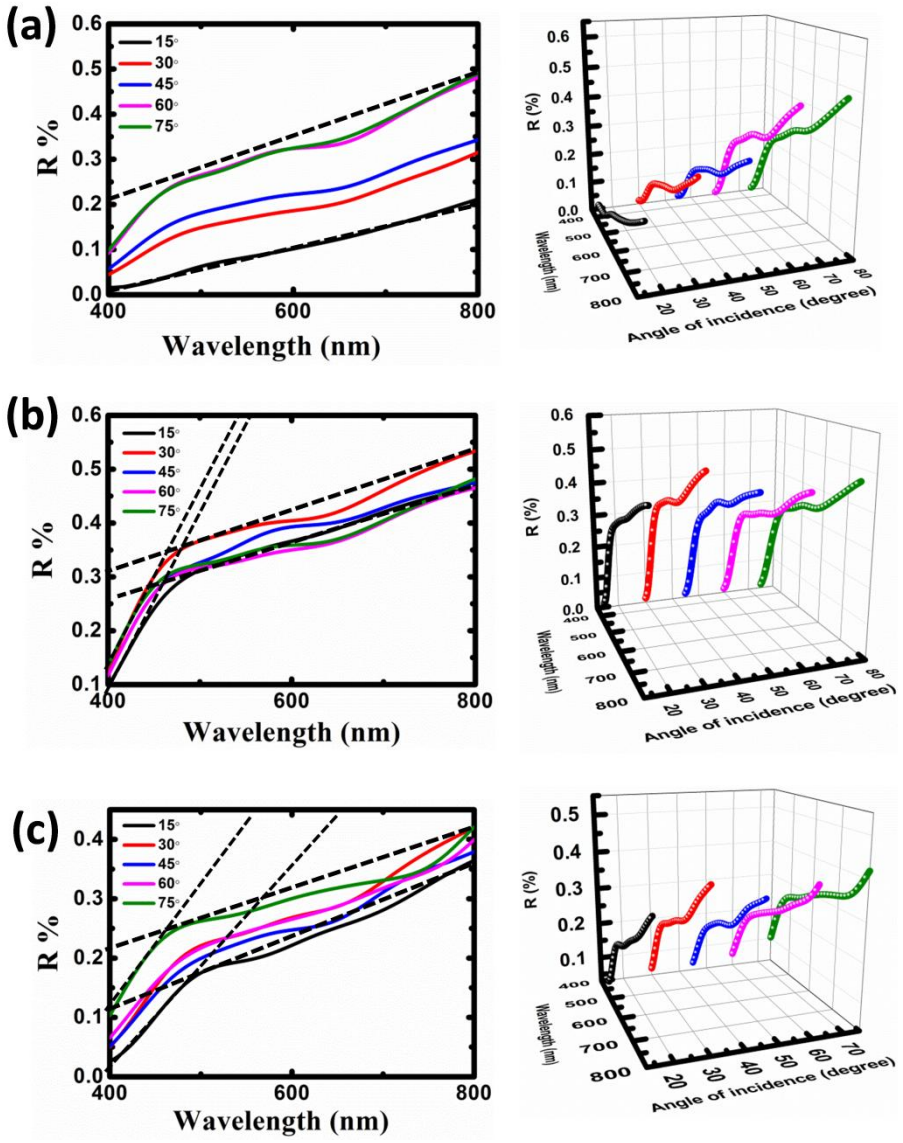

Figure 4.4B**:** 2D (left) and 3D (right) views of the reflectance spectra, revealed for the (a) WA, (b) LW, and (c) DBT butterfly specimens considered with varied angle of incidence.

The overall reflectance and the nature of bending, to a great extent, are quite similar. It is worth mentioning here that, incident angle may not necessarily affect light absorption events by pigmentary constituents, however, periodically stacked cover scales that comprise of rectangular microstructures formed out of the longitudinal ridges and cross-ribs could have markedly influenced it. The variation in reflectance curves with incident angle as displayed by the DBT

specimen was in-between the responses that of WA and LW wing parts. The dotted parallel lines imposed in each of the sub-figures are essentially to illustrate spread of the curves and nature of bending in the visible wavelength region (Fig. 4.4 B (a-c)). Schematic representation about angle dependent thin film interference and sub-surface volume scattering can be found in Fig. 4.5A.

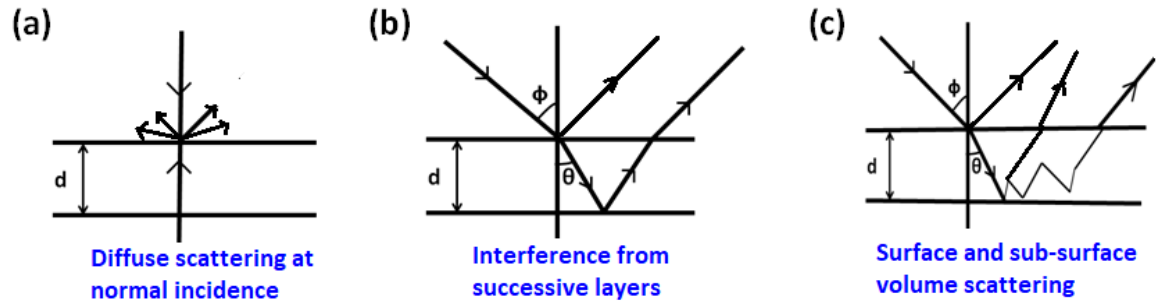

Figure 4.5A: Schematic representation of the reflected light acquired via different scattering processes.

The condition for constructive interference relevant to thin layers is, [28]

$$2d\left(n_2 - \frac{n_1^2}{n_2}\right) = m\lambda \cos\theta, \tag{4.1}$$

where $$\cos\theta = \sqrt{1 - \left(\frac{n_1}{n_2}\right)^2 \sin^2\phi}\,. \tag{4.2}$$

Here, ϕ is the angle of incidence, θ is the diffraction angle in the medium, λ is the wavelength maxima and m (=1) is the order of diffraction. The refractive indices of air and chitin material that make up the wings are respectively, n_1=1 and n_2=1.56 [29]. Considering 509 nm peak maxima under normal incidence (ϕ=0, θ=0), the optical path length estimated for the WA butterfly wing is, d=276.9 nm. Similarly, the DBT wing specimen that exhibited reflectance peak maxima at 450 nm, gives d=245.9 nm. The average width of the longitudinal ridges, as estimated from the SEM was comparable to the predicted value. However, with a varying angle of incidence, we anticipate a profound alteration in optical paths ($d \pm \Delta d$) and to a great extent; it will also depend on the light wavelength. Since

angle dependent reflectance data did not characterize any single maximum, rather gave steadily growing trend, we could employ three equispaced prime wavelengths, λ_B=450 nm (blue), λ_G=550 nm (green) and λ_R=650 nm (red). Along with these λ's, now d must be replaced by $d \pm \Delta d$ in equation 4.1. It is worth mentioning here that, thin film interference is normally deliberated for describing a definite colour pattern but not necessarily white colour. Here, we express our interest to examine the validity of the interference effect as a consequence of equitable reflectance contributions through the aforesaid λ's and knowing that, the optical path lengths would increase/decrease depending on the ϕ value at a particular λ. Accordingly, the change in d, *i.e.*, $|\Delta d|$ values have been estimated and enlisted in Table 4.2. We have concentrated on the wings of WA and DBT butterfly wings, as we noticed prominent changes in the spectra with varying angle, whereas in case of LW, there was a spectral overlapping, indicating the fact that the whitish colour is largely viewing angle independent.

The complex architecture of butterfly wings, with varied lamellar thickness over small regions of the butterfly wings offers inherent surface roughness and is essentially responsible for weakening the iridescent behaviour in the UV region [16]. Moreover, the wing scales also provide a platform for different optical effects, which include reflection from the longitudinal ridges and cross-ribs made of chitinous fibrils. Even if these micron scale ridges act as good scatterers, the presence of micro-beads on the white scales can enhance their behavior as scattering entities [30]. We invoke two distinctly different reasons to the aforementioned spectral features: A manifested optical path length as well as progressive sub-surface volume scattering in case of both WA and DBT specimens, whereas the LW wing specimen being a rich source of *pierid* pigments decorated over the well-ordered cover scales, makes it less dependent on the incident angle. The pigments can be felt on touch.

Table 4.2: Estimated optical parameters for the WA and DBT butterfly wings undergoing thin film interference

Angle of incidence (ϕ) in degrees	$cos\ \theta = \sqrt{1-\left(\frac{n_1}{n_2}\right)^2 sin^2\phi}$	$n_2 - n_1^2/n_2$	$\lvert\Delta d\rvert$ (nm)					
			WA (λ_B = 450 nm)	DBT (λ_B = 450 nm)	WA (λ_G = 550 nm)	DBT (λ_G = 550 nm)	WA (λ_R = 650 nm)	DBT (λ_R = 650 nm)
15	0.9861	0.92	35.7	3.4	17.8	50.5	71.5	104.3
30	0.9472		45.2	12.9	6.2	38.8	57.7	90.5
45	0.8914		58.9	26.7	10.4	22.0	37.9	70.7
60	0.8318		73.5	41.3	28.3	4.1	16.9	49.5
75	0.7852		84.9	193.1	42.2	9.9	0.48	32.9

Polarisation sensitive characteristics in butterfly wings have been studied on certain specimens although a clear insight is yet to be achieved [31]. Nevertheless, it was argued that the anisotropy in the scale components contribute largely to the polarization effects [31]. From the polarization dependent reflectance spectra (Fig. 4.5B(a-c)), one can invariably predict the degree of polarisation (p_z) using the popular equation [30]:

$$p_z = \frac{R_s - R_p}{R_s + R_p}, \qquad (4.3)$$

where, R_s and R_p are the strength of reflectance with *s* and *p* polarized light.

While the *s* and *p* polarized light showed wide variations in reflectance responses across the specimens, the WA wing would retain its polarization sensitivity over a broad range of wavelengths with markedly high and uniform values of p_z tending to 0.34 (Fig. 4.5B(a)). On the other hand, with a continuously varying trend over the full visible spectrum, the LW specimen offers p_z Notably, the whiteness of the LW wing specimen is highly polarization sensitive to any particular wavelength even though it is viewing angle independent as discussed above value in the range 0.12-0.18 (Fig. 4.5B(b)).

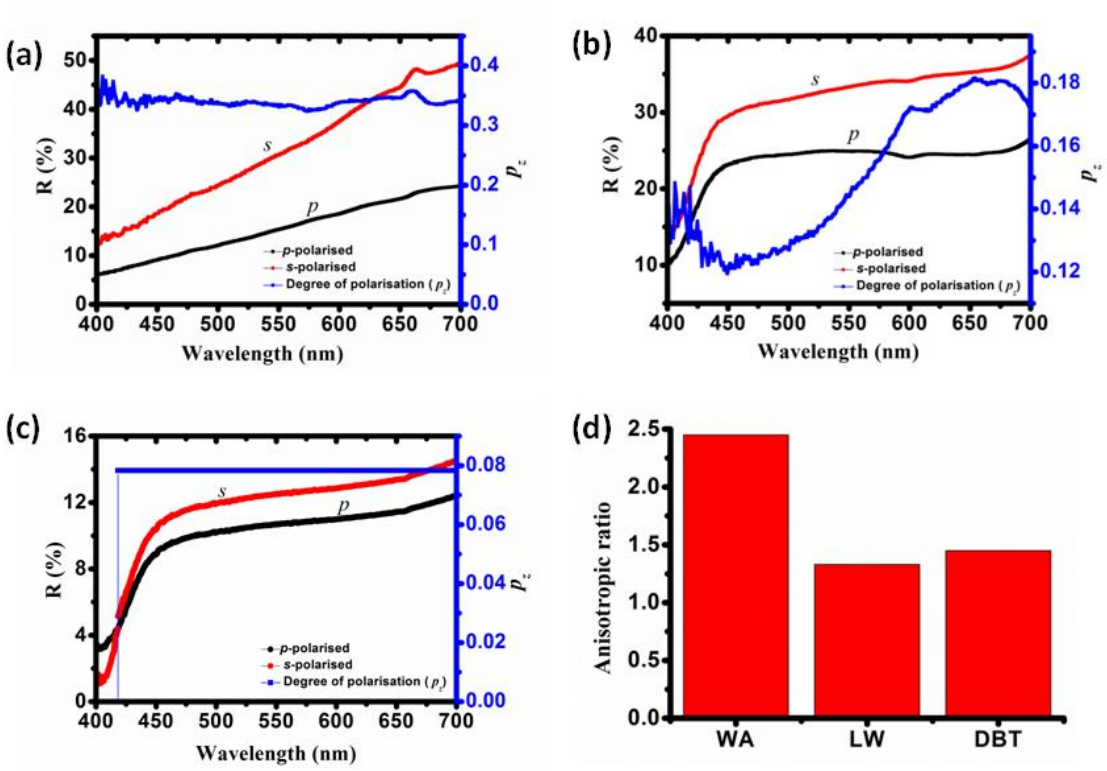

Figure 4.5B: Polarization sensitive reflectance spectra of the (a) WA, (b) LW, and (c) DBT butterfly wing specimens shown for *s* and *p*- polarized incident light. The blue-labelled curve essentially characterize respective degrees of polarization (p_z). While DBT is largely insensitive to polarization, others vary to different degree, with p_z as high as ~0.34 for the WA specimen.

As evident from Fig. 4.5B(c), the DBT specimen exhibited a substantially lowered, yet constant p_z value close to 0.08. Thus one can say that, the DBT specimen is least polarization sensitive as compared to other two wing types. We also define a characteristic parameter linked to polarization anisotropy (α_p), by dividing area under the curves between the *s* and *p*- polarized reflectance curves (Fig. 5B(d)). It is quite apparent that, the α_p value of the WA wing is relatively higher (nearly double) than the other specimens, thereby suggesting that, reflectance via strong sub-surface volume scattering is at work apart from the thin film interference.

4.5 Representative chromaticity diagrams of the butterfly wings

The remarkable difference in structural colouration can be examined with the help of chromaticity diagrams by employing principles of CIE 1931 color space [32]. The CIE diagrams essentially characterize the region (triangular gamut) bound by three primary colors, B (blue), G (green) and R (red). Thus any point within the bound region and lying on the line joining between any two primary colors will represent additive mixture in a proportionate manner. Depending on the choice of focus and identifying W (white) as the centroid, the triangular gamut can be formed by the line joining B, G and R termini. In the representative diagram the loci of the reflected wavelengths (corresponding to different intensities) are carefully considered and subsequently, the wavelength is converted to the chromaticity coordinates, x and y. Referring to the chromaticity features shown in Fig. 6(a-f), the white wing parts of the WA, LW and DBT wings display distinctly different characteristics, with and without ethanol treatments. As can be noticed, the WA wing part exhibits colour points that are accumulated around W and tending to line up towards R terminus, in a sequential manner (Fig. 4.6(a)). Upon ethanol-treatment, reflectance response gets improved due to the modulation in scattering events, and consequently, a more open distribution of the points could be perceived around B, W and R (Fig. 4.6(b)). As a consequence of enhanced reflectance, it was believed to be due to the momentary modification in the micro-morphological make-up upon adequate ethanol uptake by the scales. The LW wing part, upon ethanol-adsorption, also gave a precise distribution of colour points spread across B, W and R termini, though the points are largely concentrated along B and W line for the untreated wing part (Fig. 4.6(c) and (d)). The untreated white part of the DBT wing offers an orderly accumulation of colour points around W, away from both B and G termini but not R (Fig. 4.6(e)). In case of ethanol treated specimen, several colour points are pushed away from the R terminus, which give rise to the crowding at the periphery of the centroid W (Fig. 4.6(f)).

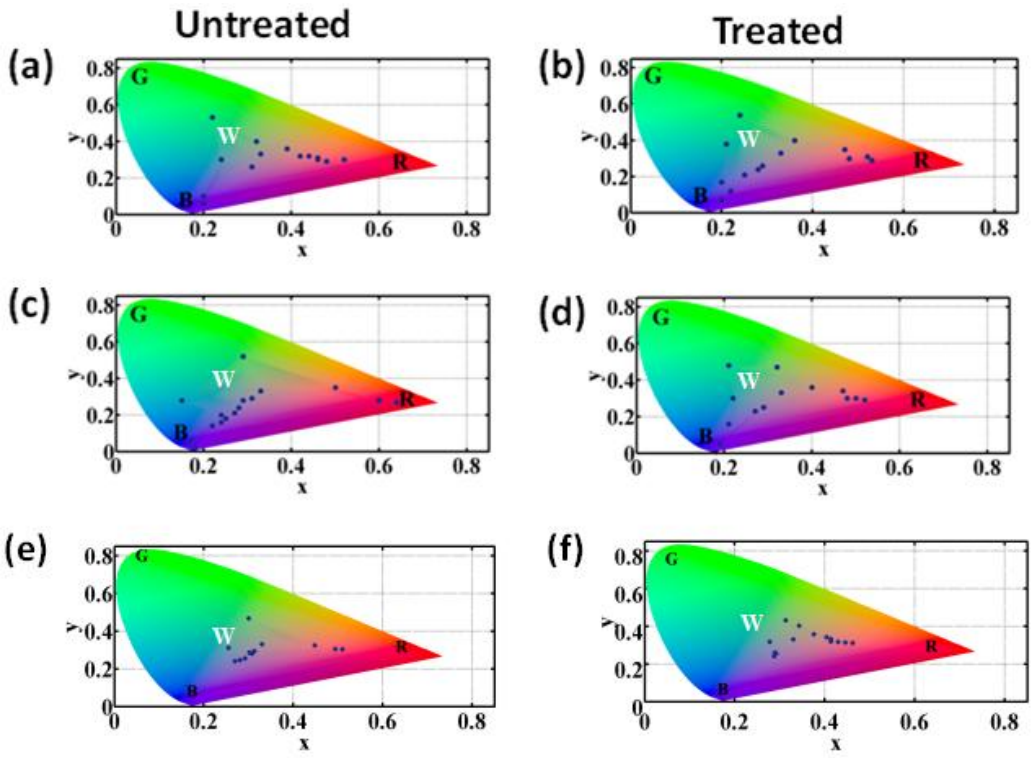

Figure 4.6: Chromaticity diagrams of the white parts of the (a,b) white admiral (WA), (c,d) large-white (LW), and (e,f) dark- blue tiger (DBT) butterfly wings. The characteristic plots, for ethanol-treated specimens, are shown in (b), (d) and (f). Note the alike distribution of color points exhibited by the WA and LW specimens.

It is worth mentioning here that, the pure LW wings have adequate powdery/pigmentary species, which one can immediately feel on touch. In fact, both LW and DBT have periodically arranged scales, but microscopically, they differ in dimensions of the intra scale elements as a result of which reflectance and consequently, chromaticity landscapes get altered.

Nevertheless, ethanol treated WA and LW wings share a common optical trend, as substantiated from both the reflectance characteristics as well as colorigrams (Fig. 4.3(h)).

4.6 Wetting de-wetting phenomena in the butterfly wings under study

Butterfly wings, in view of their precise organization of scales and complex architecture, impart not only striking structural colouration but also interesting

wettability characteristics, which vary from specimen to specimen. By employing tilting plate methodology, we examined the static and dynamic CAs of the three aforementioned butterfly specimens belonging to *Lepidoptera* order. The surface wettability can be visualized from the nature of water holding capacity at the specimen surface-structure and accordingly, the progressive development of the drop with tilting can be found in Fig. 4.7A (a-d). The length of the contact line of the water droplet on the specimens is given in Table 4.3,

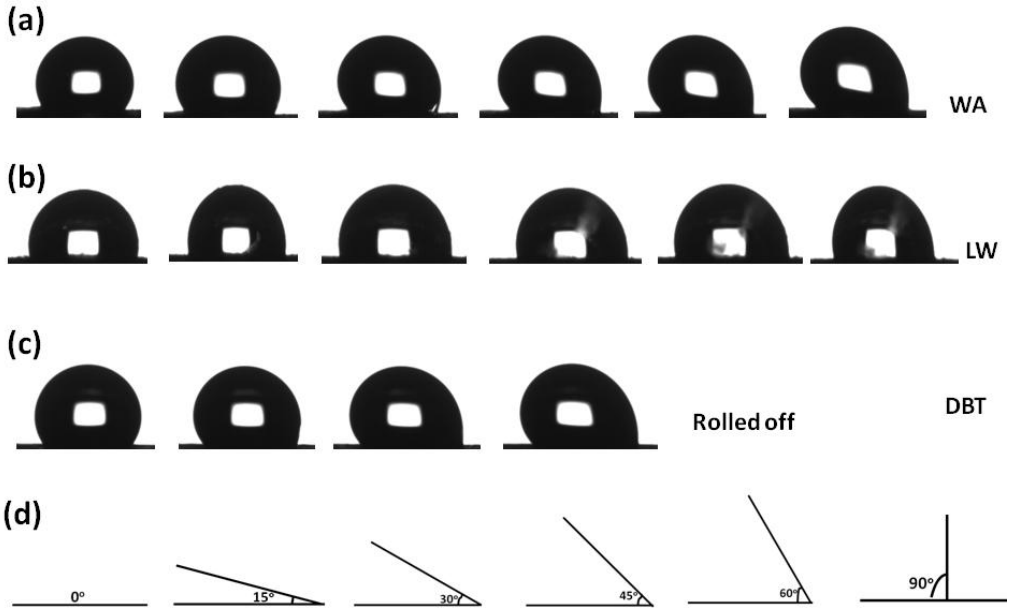

Figure 4.7A: Water droplet on the tilting plate at (a) WA (b) LW (c) DBT butterfly specimens.

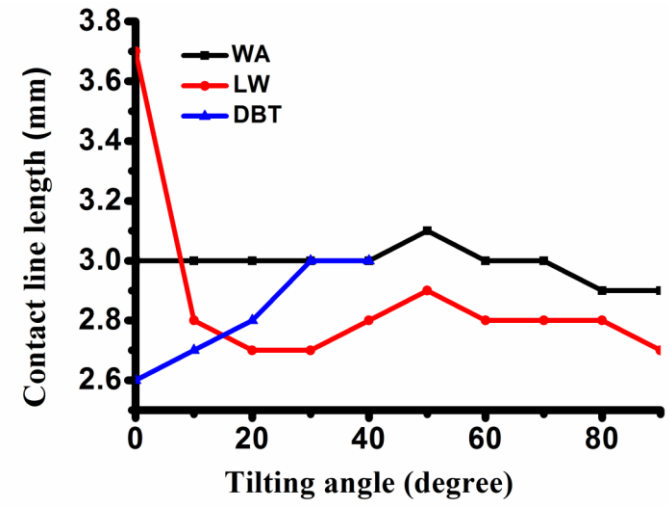

Figure 4.7B: Length of contact line on the butterfly specimens with varying tilting angle.

Table 4.3: Contact line length (mm) variation with tilting angle

Tilting angle,β (degree)	WA	LW	DBT
0	3	3.7	2.6
10	3	2.8	2.7
20	3	2.7	2.8
30	3	2.7	3
40	3	2.8	3
50	3.1	2.9	
60	3	2.8	
70	3	2.8	
80	2.9	2.8	
90	2.9	2.7	

while Fig. 4.7B depicts profiles of the contact line length with varying tilting angle. The schematic of base-tilting is shown in Fig. 4.7 A (d). Note the droplet shape at both the extremes. In fact, the tilting plate methodology is considered as a reliable method for evaluating dynamic CAs as well as contact angle hysteresis (CAH), which offer deterministic roles in the wetting-dewetting transition [33]. When a liquid droplet makes contact with a rough, inclined surface, it does not have a single equilibrium CA value but have several characteristic CAs, termed as advancing (θ_{adv}) and receding (θ_{rec}) angles.

They are also recognized as maximum and minimum values while discussing as regards, base-tilting. With tilting of the base the nature of the droplet becomes extremely dynamic and we define, CAH=θ_{adv} -θ_{rec}. As can be found in Fig. 4.8(a-c), note the nature of optimum CAs exhibited by the WA, LW and DBT wings with base-tilting. The average maxima and minima CAs are predicted through the contact lines by way of extrapolating global optimal values backward in *y*-axes, shown by dotted lines. The representative CAH histograms of the three butterfly specimens are presented in Fig. 4.8(d), which portray observably low CAH of the LW butterfly wing (Table 4.4A). Interestingly, the droplet rolls off the DBT wing- surface as the base-tilting was increased beyond 50^0 (Fig. 4.7 A(c)).

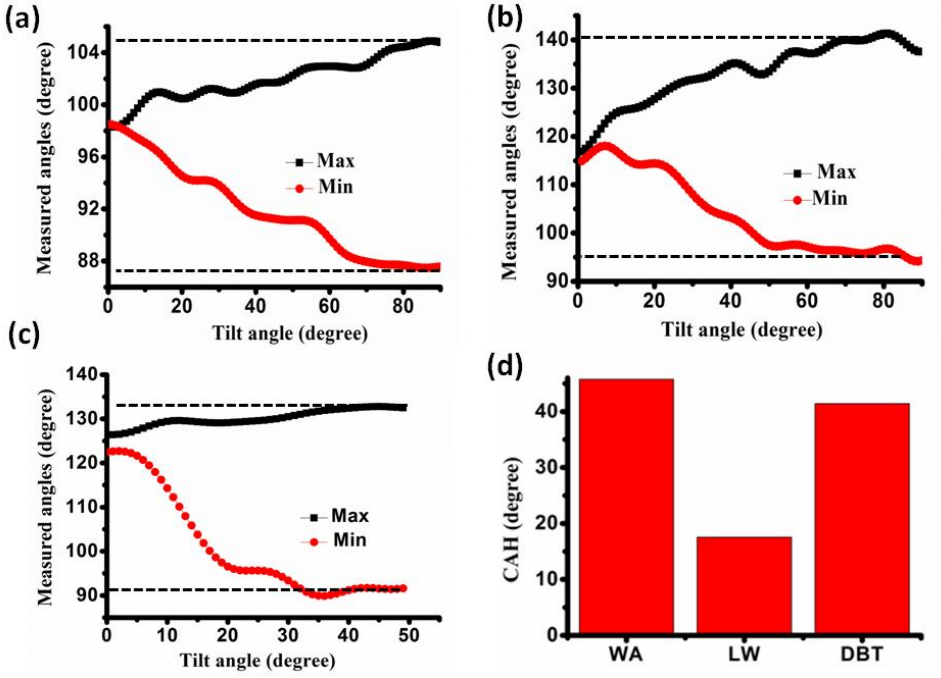

Figure 4.8: Advancing and receding angles of the (a) WA (b) LW (c) DBT and (d) histogram representation of the CAH.

This was believed to be due to a relatively low water-solid fraction, high CA and CAH that gave rise to low adhesion for much inclined surfaces. The CAH values essentially specify the extent of adhesion of the water droplet on the solid-surface, while tilting does have an influence due to variation in local surface roughness. The rough scales of the butterflies, in fact, impart hydrophobicity as evidenced from the wettability feature of the butterflies belonging to *Nymphalidae* family possessing short scales [34]. Here, both WA and DBT specimens, which belong to *Nymphalidae* family exhibited high CA as compared to their LW counterpart that fits in *Pieridae* family. Using Wenzel and Cassie-Baxter equations [35, 36] which basically describe the collapsed and suspended states; respectively one can estimate the roughness factor, r_φ and solid-water fraction, φ as discussed for dragonflies in the previous chapter. To a great extent, the whole butterfly wing comprises of chitin which normally gives a static CA in the range 100-105° [34, 37]. Fang *et. al.* have hypothesized three models based on the scale structure of the wing [34]. The first model essentially emphasizes micro-class roughness that arises as result of regular, flat scales arranged in a periodic manner.

Here hydrophobicity was believed to increase when the separation between the scales is larger than the width of the scale itself. The second model is based on the presence of vertical gibbosities with triangular cross sections that line up periodically in each of the scales and therefore, it could feature sub-micron scale surface roughness. Finally, the third model prescribes effective contact angle, θ_t as a consequence of combinatorial effect of both micro-class and sub-micron scale features formulated as,

$$\cos\theta_t = \frac{be}{cf}\left(r_\varphi \cos\theta + 1\right) - 1, \quad (4.4)$$

where, $r_\varphi = \sqrt{\frac{4d^2}{e^2} + 1}$ is the roughness factor (4.5)

and $\frac{be}{cf}$ is the water-solid fraction

It was known that, surface roughness describes the ratio between actual area to the projected area. The symbols *b*, *c*, *d*, *e* and *f* used here refer to width of the scale, distance between consecutive scales, width of the vertical gibbosity, height of the gibbosity and separation between them; respectively (Fig. 4.9).

For dual-roughness surface comprising of both micro and nanoroughness has been described where six different modes of hydrophobicity have been proposed [38], as mentioned in *Chapter I*. In the butterfly scales, we observe the presence of both micron and sub-micron scale roughness. The equations for the Cassie-Cassie, Cassie-Wenzel, Wenzel-Cassie, Wenzel-Wenzel modes, as mentioned in *Chapter I* can be slightly modified by replacing φ_n by $\varphi_{m'}$ and r_n by $r_{m'}$, where $\varphi_{m'}$ and $r_{m'}$ are solid-water fraction and roughness factor for the sub-micron roughness. Here, microroughness can be calculated from: $r_m=\sqrt{(1+b^2/4a^2)}$ and φ_m=b/c, $\varphi_{m'}$=e/f.

Using the modified equations we have calculated the theoretical CA for all the modes, as enlisted in Table (4.4 A, B) below. Among the three specimens, DBT butterfly offers a higher static CA of 123°, in contrast to higher adhesion to the water droplet, which is in accordance to the rose-petal effect but only existed only upto 50° angle of base-tilting.

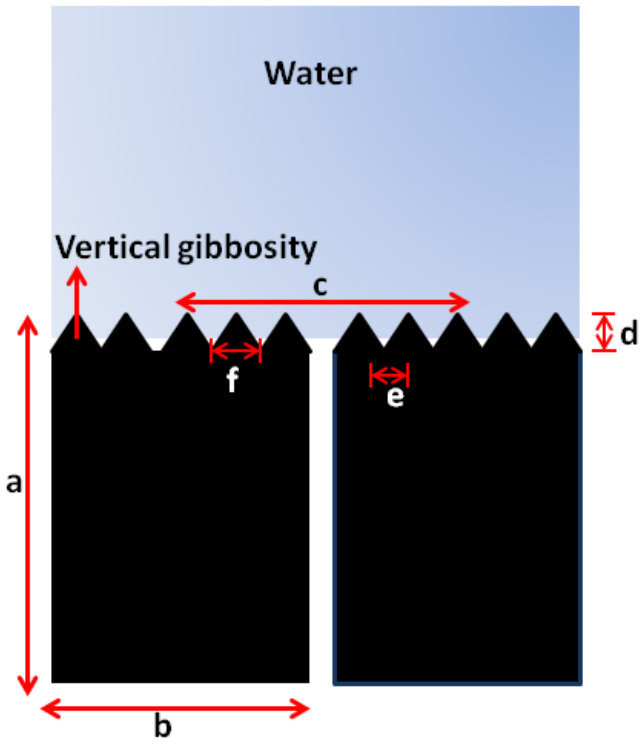

Figure 4.9: Schematic representation of the butterfly scale arrangement with micron and sub-micron scale roughnesses latter being prominent due to presence of vertical gibbosities.

At β=50°, the droplet rolls off the wing surface, showing superhydrophobicity. Morphologically, DBT wing consists of two types of scale, and also cross ribs are connected in a complicated fashion as compared to the WA and LW specimen, thus exhibiting higher CA value. We have observed that the height of the gibbosity is maximum for WA butterfly and least for LW butterfly specimen. Also, in an individual scale, the presence of vertical gibbosities is more prominent in WA butterfly wing. The characteristic parameters are enlisted in the Table 4.4A and B.

Table 4.4A: Static CA, roughness factor, water-solid fraction, advancing, receding angles, CAH, along the theoretical CA

Sample	Static CA (deg.)	r_φ	φ	Adv. Angle (deg.)	Rec. angle (deg.)	CAH (deg.)	Theoretical roughness factor	Theoretical water-solid fraction	Theoretical CA (deg.) (model 3)
WA	120.6	2.9	0.59	141.25	95.49	45.76	1.12	0.67	121
LW	100	1.0	0.99	104.92	87.36	17.56	1.37	1.08	100.19
DBT	123.3	3.16	0.54	132.73	91.30	41.43	1.17	0.47	128.71

Table 4.4B: The scale parameters, along with micron and sub-micron roughness factor and water-solid fractions. The CA measured according to C-C, C-W, W-C, W-W modes are also given below

a (μm)	b (μm)	*c* (μm)	*d* (μm)	*e* (μm)	*f* (μm)	r_m	$r_{m'}$	φ_m	$\varphi_{m'}$	C-C	C-W	W-C	W-W
111.5 ±3.4	52.45 ± 4.7	65.92 ±1.3	7.34± 0.7	16.48 ±1.2	17.96 ±2.3	1.02	1.33	0.79	0.91	113.8	113.1	104.5	103.5
91.44 ±2.8	46.0 ± 2.2	51.6 ±3.2	7.2± 0.2	27.6± 2	28± 3.4	1.03	1.12	0.89	0.98	106.2	106.4	101.2	101.5
91.85 ±2.3	56.4± 2.5 (thick scales)	88±7. 3	14.48 ±0.3	20.8± 3.5	21.4± 2.4	1.04	1.71	0.64	0.97	119.14	123.3	101.8	107.6

4.7 Conclusion

In this work, we have studied the colour in three butterfly specimens with whitish appearance along with their wettability properties. A qualitative investigation on the whitish structural coloration has been made by employing micro-morphological and reflectance characteristics. The white-appearing parts of the three important butterfly specimens belonging to the *Lepidoptera* order were studied as regards, their microstructural build up, incident angle dependent reflectance and polarization sensitivity features. Structurally, the white parts of the three wing types were diverse, but in the white admiral wing-type, the scales while arranged in an aperiodic manner with void spaces filled by the micro-beads. Moreover, surface roughness mediated multi-scattering events in the white part of the WA specimen is mainly responsible for displaying a

higher reflectance response as compared to the brown part that has more organized scales. In contrast, pterin based pigmentary contribution was quite significant in the LW wing specimen which showed a minimal dependence of the reflectance feature to incident angle variation and therefore, color should be viewing angle independent. In this case, a fall in reflectance after ethanol-treatment was attributed to adequate adsorption response by pterin pigments. Unlike the WA wing specimen, both the LW and DBT wings showed lowered reflectance features after ethanolic adsorption by scales. As an imperative finding, upon ethanol uptake, the white parts of both the wing-types shared a common reflectance feature in the long wavelength regime. We have observed that, the LW and DBT butterfly tend to exhibit stronger responses in case of without ethanol treatment than the case with treatment. The whole study has led us to a very interesting conclusion that not only the arrangement of microstructure but also the difference in refractive indices between the chitinous microstructure would matter and accordingly, its surrounding environment is largely responsible for the structural color manifestation. Angle dependent studies provide additional information as regards, the underlying mechanism responsible for white-appearing structural color in the specimens under study. It is the thin film interference and sub-surface volume scattering that are anticipated in WA and DBT wing-types, whereas, the LW wing contributes largely through pterin pigments. Polarisation-sensitive reflectance studies have revealed that, DBT is less sensitive to polarization as compared to WA and LW wings. While p_z (~0.34) is quite uniform all over the visible spectrum in WA specimen, it was found be modulated up to 0.18 in case of the whole-white LW wing-type. The viewing angle dependency, polarization sensitivity and their modulation effects would help visualizing artificial designs, coatings and camouflage in specific applications. From the wettability features, as studied, we have found that DBT shows higher static CA of 123.3° and a roll-off angle at 50°. Whereas, the WA and LW exhibits CA of 120.6° and 100° respectively and the liquid droplet was pinned to the surface without rolling-off.

References

[1] Kinoshita, S. *Structural Colors in the Realm of Nature*, World Scientific Publishing, Singapore, 2008.

[2] Stavenga, D. G., Stowe, S., Siebke, K., Zeil J., Arikawa, K. Butterfly wing colours: scale beads make white pierid wings brighter. *Proceedings of the Royal Society London B*, 271:1577-1584, 2004.

[3] Brink J. L., Lee, M. E. Confined blue iridescence by a diffracting microstructure: an optical investigation of the *Cynandra opis* butterfly. *Applied Optics*, 38:5282-5289, 1999.

[4] Ghiradella, H., Aneshansley, D., Eisner, T., Silberglied, R., Hinton, H. E. Ultraviolet reflection of a male butterfly: Interference color caused by thin-layer elaboration of wing scales. *Science*, 178:1214-1217, 1972.

[5] Biró, L. P., Bálint, Zs, Kertész, K., Vértesy, Z., Márk, G. I., Horváth, Z. E., Balázs, J., Méhn, D. Lousse, V., Kiricsi, I., Vigneron, J. P. Role of photonic-crystal-type structures in the thermal regulation of a Lycaenid butterfly sister species pair

Physical Review E, 67:021907, 2003.

[6] Kertész, K., Bálint, Z., Vértesy, Z., Márk, G., Lousse, V., Vigneron, J.P., Rassart, M., Biró, L.P., Gleaming and dull surface textures from photonic-crystal-type nanostructures in the butterfly Cyanophrys remus. *Physical Review E*, 74:021922, 2006.

[7] Miaoulis, N., Wong, P.Y., Heilman, B.D. The effect of microscale and macroscale patterns on the radiative heating of multilayer thin-film structures. *Microscale Heat Transfer*, *ASME Heat Transfer Proceedings Series*, 291:27-34, 1994.

[8] Tada, H., Mann, S.E., Miaoulis, I.N., Wong, P.Y. Effects of a butterfly scale microstructure on the iridescent color observed at different angles. *Optics Express*, 4:87-92, 1999.

[9] Chung, K., Yu, S., Heo, C-J, Shim, J.W., Yang, S-M, Han, M. G., Lee, H-S, Jin, Y., Lee, S.Y., Park, N., Shin, J-H, Flexible, angle-independent, structural color

reflectors inspired by morpho butterfly wings. *Advanced Materials*, 24, 2375 (2012).

[10] Land, M.F. The physics and biology of animal reflectors. *Progress in Biophysics and Molecular Biology*, 24:75-106, 1972.

[11] Wong, P.Y., Miaoulis, I.N., Tada, H., Mann, S. Selective multilayer thin-film development in insects. *ASME Fundamentals of Microscale Biothermal Phenomena*, 1997.

[12] Ingram, A.L., Parker, A.R. A review of the diversity and evolution of photonic structures in butterflies, incorporating the work of John Huxley (The Natural History Museum, London from 1961 to 1990). *Philosophical Transactions of Royal Society B*, 363:2465-2480, 2008.

[13] Bálint, Z., Kertész, K., Piszter, G., Vértesy, Z., Biró, L.P. The well-tuned blues: the role of structural colours as optical signals in the species recognition of a local butterfly fauna (Lepidoptera: Lycaenidae: Polyommatinae). *Journal of Royal Society Interface*, 9:1745-1756, 2012.

[14] Siddique, R.H., Vignolini, S., Bartels, C., Wacker, I., Hölscher, H. Colour formation on the wings of the butterfly Hypolimnas salmacis by scale stacking. *Scientific Reports*, 6:36204, 2016.

[15] Shevtsova, E., Hanssona, C., Janzen, D.H., Kjaerandsen, J. Stable structural color patterns displayed on transparent insect wings. *Proceedings of the National Academy of Sciences of the United States of America*, 108:668-673, 2011.

[16] Stavenga, D.G., Giraldo, M.A., Hoenders, B.J. Reflectance and transmittance of light scattering scales stacked on the wings of pierid butterflies. Optics Express, 14: 4880-4890, 2006.

[17] Yan, F., Gang, S., TongQing, W. Qian, C., LuQuan, R. Hydrophobicity mechanism of non-smooth pattern on surface of butterfly wing. *Chinese Science Bulletin*, 52:711-716, 2007.

[18] Biró L.P., Vigneron, J.P. Photonic nanoarchitectures in butterflies and beetles: valuable sources for bioinspiration. Laser & Photonics Reviews, **5**:27-51, 2011.

[19] Gilbert, L.E., Forrest, H.S., Schultz, T.D., Harvey, D.J. Correlations of ultrastructure and pigmentation suggest how genes control development of wing scales of Heliconius butterflies. *The Journal of Research on the Lepidoptera*, 26**,** 141-160, 1988.

[20] Stavenga, D.G., Leertouwer, H.L., Wilts, B.D. Coloration principles of nymphaline butterflies – thin films, melanin, ommochromes and wing scale stacking. *Journal of Experimental Biology*, 217:2171-2180, 2014.

[21] Wijnen, B., Leertouwer, H.L., Stavenga, D.G. Colors and pterin pigmentation of pierid butterfly wings. *Journal of Insect Physiology*, 53:1206-1217, 2007.

[22] Wilts, B.D., Wijnen, B., Leertouwer, H.L., Steiner, U., Stavenga, D.G. Extreme Refractive Index Wing Scale Beads Containing Dense Pterin Pigments Cause the Bright Colors of Pierid Butterflies. *Advanced Optical Materials*, 5:1600879, (8 pp.), 2017.

[23] Wilts, B.D., Sheng, X., Holler, M., Diaz, A., Guizar-Sicairos, M., Raabe, J., Hoppe, R., Liu, S-H, Langford, R., Onelli, O.D., Chen, D., Torquato, S., Steiner, U., Schroer, C.G., Vignolini, S., Sepe, A. Evolutionary-Optimized Photonic Network Structure in White Beetle Wing Scales**.** *Advanced Materials*, 30:1702057, 2018.

[24] Yoshioka, S., Kinoshita, S. Structural or pigmentary? Origin of the distinctive white stripe on the blue wing of a *Morpho* butterfly. *Proceedings of the Royal Society B*, 273:129-134, 2006.

[25] Johnsen S., Widder, E. A. The physical basis of transparency in biological tissue: ultrastructure and the minimization of light scattering. *Journal of Theoretical Biology*, 199:181-98, 1999.

[26] Aideo, S.N., Haloi, R., D. Mohanta, Exploring structural colour in uni- and multi-coloured butterfly wings and Ag^{+} uptake by scales. *Europhysics Letters*, 119:66003 (7 pp.), 2017.

[27] Niu, S.C., Li, B., Ye, J. F., Mu, Z.Z., Zhang, Z.Q., Liu, Y., Han, Z.W. Angle-dependent discoloration structures in wing scales of *Morpho Menelaus* butterfly. *Science China Technological Sciences*, 59:749-755, 2016.

[28] Simmons, J.H., Potter, K.S. *Optical Materials* (Academic Press, 2006) pp.184.

[29] Deparis, O., Vandenbem, C., Rassart, M., Welch, V.L., Vigneron, J.-P. Color-selecting reflectors inspired from biological periodic multilayer structures. *Optics Express*, 14:3547-3555, 2006.

[30] Zhao, Q., Guo, X., Fan, T., Ding, J., Zhang, Di., GuoZhao, Q. Art of blackness in butterfly wings as natural solar collector. *Soft Matter*, 7:11433-11439, 2011.

[31] Yoshioka, S., Kinoshita, S. Single-scale spectroscopy of structurally colored butterflies: measurements of quantified reflectance and transmittance. *Journal of the Optical Society of America A*, 23:134-141, 2006.

[32] CIE (1932). Commission internationale de l'Eclairage proceedings, Cambridge: Cambridge University Press

[33] Ahmed, G. Sellier, M., Jermy, M., Taylor, M. Modeling the effects of contact angle hysteresis on the sliding of droplets down inclined surfaces. *European Journal of Mechanics-B/Fluids*, 48:218–230, 2014.

[34] Yan, F., Gang, S., TongQing, W., Qian, C., LuQuan, R. Hydrophobicity mechanism of non-smooth pattern on surface of butterfly wing. *Chinese Science Bulletin*, 52:711-716, 2007.

[35] Wenzel, R.N. Resistance of solid surfaces to wetting by water. *Industrial & Engineering Chemistry*, 28:988-994, 1936.

[36] Cassie, A.B.D. Contact angles, *Discussions of the Faraday Society*, 3:11-16, 1948.

[37]Holdgate, M.W. The Wetting of Insect Cuticles by Water. *Journal of* Experimental *Biology*, 32:591-617, 1955.

[38] Cha,T-G., Yi, J. W., Moon, M-W., Lee, K-R., Kim, H-Y., Nanoscale Patterning of Microtextured Surfaces to Control Superhydrophobic Robustness. *Langmuir*, 26:8319–8326, 2010.